Conceptual monopile and tower sizing for the IEA Wind Task 37 Borssele reference wind farm

Michael K. McWilliam, Anand Natarajan, Nicolò Pollini, Katherine Dykes

Technical University of Denmark, Department of Wind Energy, Frederiksborgvej 399, 4000 Roskilde, Denmark

E-mail: `mimc@dtu.dk`

Garrett E. Barter

National Renewable Energy Laboratory, Golden, CO 80401, USA

Abstract. This paper explores the preliminary design of the support structures for the IEA Wind Task 37 reference wind farm at the Borssele site III and IV. The study looks at two different design methods that might be used within larger wind farm system design optimization (*i.e.* lay-out, electrical systems, *etc.*). The first consists of a scaling tool that scales a detailed design according to the rated power, water depth, hub height and rotor diameter. The second is a physics-based optimization approach that relies on the WISDEM$^{\circledR}$ design tool. This research compares the results of these two methods for the design of both the tower and monopile of the IEA 10-MW and 15-MW reference wind turbines at a range of sea depths (25 m, 30 m, 35 m, 40 m). The two tools yield very similar results in terms of monopile base diameter, support structure natural frequency and mass. WISDEM is then used to also investigate the sensitivity of the design to the tower top forces, wave conditions and the soil conditions. It is shown that tower top forces dominate the design. In general, large diameter structures can carry additional costs associated with manufacturing and transportation requirements. Thus, the paper is concluded with a trade-off study between mass and diameter that quantifies the effect of the reduction in monopile diameter with the increase in structural mass.

1. Introduction

The design of wind farms seeks to optimize the overall profitability by trading off system performance and cost while meeting prescribed design objectives and constraints. Wind farm design involves many interacting engineering and scientific disciplines (aerodynamics, structural mechanics, meteorology, civil engineering *etc*) along with the design, placement and sizing of many components (the wind turbine, tower, support structure, lay-out, electrical collection *etc.*). Traditionally, engineers have used a sequential approach where each aspect of the design is considered separately. However, Perez-Moreno [1] has shown that an integrated design optimization approach can lead to better solutions than a sequential approach by taking advantage of the different couplings. Kallehave *et. al.* [2] has also argued that an integrated approach is important for achieving the greatest cost reductions.

Due to the complexity of a larger integrated optimization, it is not necessarily feasible to perform the sub-component design to the same level of fidelity as one would use in a sequential

design process. Thus, there is a need for simple sizing tools that can be integrated within larger system optimizations. This paper looks specifically at such tools for the design and sizing of towers and monopiles.

The design of offshore wind turbine support structures has received a lot of research attention. Muskulus and Schafhirt [3] has given an extensive review that looked at all the different aspects and challenges of this design problem and the different methods that have been demonstrated within the literature. They highlight the importance of integrating fatigue and the large computational costs due to the many simulations required to cover all the different wind, wave and fault conditions. While Kallehave *et. al.* [2] has also given a broad overview of the support structure design problem from an industrial perspective, highlighting several areas that can reduce costs. They highlight how position specific design and automated optimization methods have provided significant cost savings for industry.

Other researchers have given more detailed investigations on mono-pile design. Morato *et. al.* [4] performed a detailed investigation into the Design Load Cases (DLCs) that most responsible for the design driving loads to reduce the overall analysis loads within iterative design processes. While, Velarde and Bachynski [5] explored the use of monopiles in deeper sees using high fidelity finite element method (FEM). They found that the sea-states play an increasing role in the fatigue damage, with increasing sea depths.

Finally, on the topic of support structure design methodology, Chew *et. al.* [6] has demonstrated a fairly high fidelity design optimization that uses gradient based optimization and fully coupled aero-elastic time domain analysis of the wind turbine. They have demonstrated that this approach can yield significant weight savings, while at the same time due to the large number of constraints typically converge towards a point that appears to be the global optimum. While Arany *et. al.* [7] provides a comprehensive heuristic approach, based on the minimal amount of data, for developing an initial design in 10 steps. The paper highlights how the different information impacts an iterative design procedure for both the tower and foundation.

This paper demonstrates and compares two tower and monopile sizing tools. The first developed at DTU is a scaling tool that scales a detailed design according to the turbine size and water depth. While the second is the physics based optimization tool Wind Plant Integrated System Design and Engineering Model (WISDEM®) [8] developed by NREL. The WISDEM support structure design capabilities have already been demonstrated by Damiani and Dykes [9]. There are differences in the level of fidelity between these two tools. The original detailed designed that is used in the DTU scaling tool is at a higher level of fidelity than the analysis within WISDEM. Nevertheless, physics-based optimization is a much higher fidelity approach than scaling for generating new optimized designs. An important weakness for both approaches is the lack of fatigue considerations, despite this limitation both tools can still provide some insights in tower and monopile sizing from a systems perspective. Furthermore, extending both of these tools with fatigue damage estimation is a subject of future work for both.

The International Energy Agency (IEA) Wind Task 37 on systems engineering has developed a reference wind farm located in the Borssele offshore wind project areas III and IV [1]. Furthermore, the tasks has also developed a new 10-MW reference turbine [10], and a 15-MW reference turbine [11, 12] which will be used within this study.

Design engineers may only have access to historical wind and wave data. Furthermore, due to costs, the assumed soil conditions must be estimated based on sparse sampling. To understand the impact of this uncertainty, this article also provides a sensitivity study of the environmental conditions on the final optimized designs within WISDEM. This uncertainty study is not an evaluation of how robust a fixed design is to site uncertainty, but it is rather an analysis of how the variability of the input parameters affects the final design.

The overall size of the components is another major factor in the costs associated to the manufacturing and logistic challenges of the offshore wind energy industry. To minimize the

material costs, in principle one would want to minimize mass. Yet this can lead to structures with large diameters that may further increase the manufacturing and logistic costs. To explore this aspects, this paper explores the extent to which the maximum diameter can be reduced without significant increases in the structural mass.

The paper is organized as follows: First, the two design methods are summarized in Sec. 2. Sec. 3 provides the details of the turbine and site data used in this work. In Sec. 4 the numerical results for different studies are discussed. The paper concludes with a short discussion on possible future work in Sec. 6, and brief final remarks in Sec. 5.

2. Design methods

2.1. DTU scaling tool

The DTU monopile scaling tool is based on a detailed design of a large monopile for the DTU 10-MW reference wind turbine [13]. The background of the monopile design for the reference wind turbine is given in [14]. The tool is based on scaling the design developed in [14] according to the rated power of the turbine (see Eq. (1)). The thickness is scaled linearly according to this factor times the ratio of the actual rotor diameter to the rotor diameter scaled from the baseline 10-MW turbine (see Eq. (2)). The support structure diameter is a free variable in the optimization. The scaling can be modified to accommodate different hub heights, water depths and geometric constraints. In this work, only the water depth was varied. Varying water depths are incorporated into the scaling by shifting the z ordinate as shown in Eq. (3). Within this tool, the z ordinate starts at the base of the monopile, so this shift merely extends the base of the monopile. The tool has checks on the frequency (see Eq. (4)). The Excel optimization solver GRG Nonlinear that is built into MS Excel is used to minimize the mass, with the diameters of the different sections of the support structure being the optimization variable. The lower limit of the natural frequency is a constraint set to be above the rotational speed of the rotor (1P frequency). The diameter of the support structure is constrained to be monotonically reducing with height. The diameter constraints in the Excel tool and WISDEM are set to the same limits as provided below. This scaling tool uses the ratio of the square root of the rated power capacities of two turbines as the basic scaling variable to size the support structure. Along with this scaling parameter, the vertical stations of the support structure for the new turbine are also modified to account for the blade tip-water clearance, water depth and soil depth. The basic scaling parameters are given below as:

$$S = \sqrt{\frac{P}{P_{\text{ref}}}} \qquad (1)$$

$$t = t_{\text{ref}} * S * \frac{D}{D_{\text{scaled}}} \qquad (2)$$

$$z_i = z_{\text{ref},i} * S + (d - d_{\text{ref}}) \qquad \forall i > 1 \qquad (3)$$

$$f = \frac{1}{2\pi} \sqrt{\frac{3\frac{1}{N}\sum_{i=1}^{N} E_{\text{ref},i} I_{\text{ref},i}}{m_{tt} L^3}} \qquad (4)$$

where, P is the power, z is the vertical height, d is the water depth for the monopile sections, EI is the bending rigidity, L is the total height of the support structure and m_{tt} is the tower top mass.

2.2. WISDEM

The monopile and tower design problem can be specified as the following mass (m) minimization problem, where $\boldsymbol{d}_t$, $\boldsymbol{t}_t$, $\boldsymbol{d}_m$ and $\boldsymbol{t}_m$ are the tower diameter and thickness, then monopile diameter and thickness, respectively. Both the tower and the monopile are constructed with 3 sections each. Thus, there are 6 thickness design variables, 1 for each section and 7 diameter design variables, 1 each for the ends of the sections. The structure is constrained by a stress constraint

($i.e.$, $\sigma < \sigma_y$), constraints on the frequency for a soft-stiff design ($i.e.$, f_1 and f_2 between 1P and 3P with a margin of $\delta f = 5\%$) and then both shell buckling ($i.e.$, n_s) and global buckling ($i.e.$, n_g) constraints. Additional geometric constraints were applied to limit the amount of taper and ensure that the monopile tower structure reduced in diameter monotonically from top to bottom. The tower and monopile are manufactured with structural steel.

$$
\begin{aligned}
\underset{\boldsymbol{d_t}, \boldsymbol{t_t}, \boldsymbol{d_m}, \boldsymbol{t_m}}{\text{minimize}} \quad & m \\
\text{s.t.} \quad & 3.87\,m < d < 9\,m \quad \text{(for the 10-MW)} \\
& 3.87\,m < d < 10\,m \quad \text{(for the 15-MW)} \\
& 0.004\,m < t < 0.2\,m \\
& \sigma < \sigma_y \\
& f_{1p} + \delta f < f_{1,2} < f_{3p} - \delta f \\
& n_{s,g} < 1.0
\end{aligned}
\tag{5}
$$

There are two load cases (DLCs) considered in this design problem:

DLC 1.6 Maximum rotor thrust ($i.e.$, rated wind conditions) and maximum wave loading (50-yr)

DLC 6.1 Wind turbine idling during an extreme 50-yr wind and wave event

The design will be based on site conditions of the Borssele site III and IV. At this site, water depths range from 25–40 m, and a range of designs will be produced for 25 m, 30 m, 35 m and 40 m water depths. Furthermore, the wind and wave conditions will be based on this site as well.

The tower/monopile analysis and optimization is based on a finite-element structural model using linear beam elements. The schematic of the model is shown in Fig. 1. The rotor nacelle assembly (RNA) is modelled as a lumped mass with a concentrated force applied to the tower top. Additionally, the transition piece is also modelled as a concentrated mass. The load cases are based on static analysis. Eigen value analysis is used to determine the fundamental frequencies. The model also accounts for the aerodynamic drag of the wind and waves. The soil is modelled as a stiffness applied at the base of the monopile. The structural elements are modelled as tapered cylinders with a geometry shown in Fig. 1. The WISDEM analysis calculates the constraint values for material stress, shell buckling and global buckling. Each of these aspects will be described briefly in turn.

Figure 1: Schematic of the model

The structural model within WISDEM is based on the open-source FEM package Frame3DD [15]. The model is based on standard linear beam elements with Timoshenko shear stiffness and and has the option to include nonlinear geometric stiffness. Frame3DD can perform static and modal analysis. The details of this model and the cylindrical cross-section stiffness equations are given in [15]. The stress calculation includes the hoop stress model from the Eurocode standards
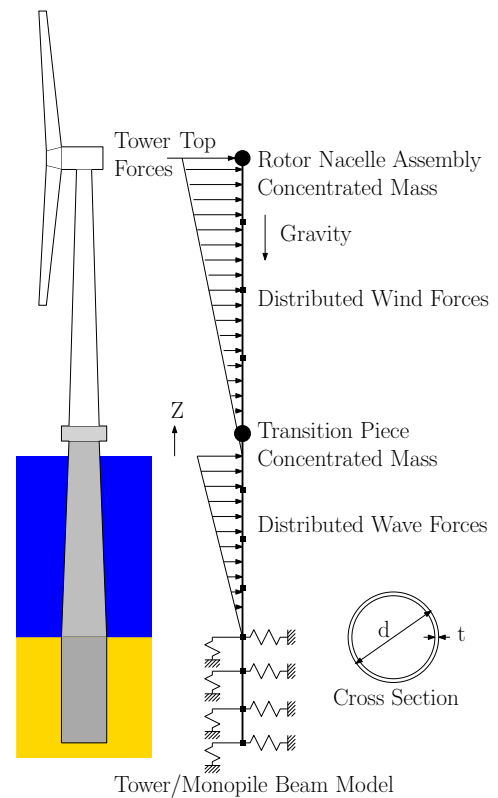
[16], while the stress constraint is based on the von Mises failure criteria. The shell buckling constraint is based on the Eurocode standards [16]. The global buckling constraint is based on the global buckling model taken from the Germanischer Lloyd design standards for offshore wind turbines [17]. All the structural constraints include safety factors and are normalized so that the constraint limit occurs at 1.

The drag forces from the wind are based on Eq. (6), where ρ_a is the density of the air, U_a is the velocity of the wind, Re_a is the Reynolds number for the wind and β is the angle of the wind. The Reynolds number is defined in Eq. (7), where μ is the dynamic viscosity. A power law wind profile was used, with a shear exponent of 0.14.

$$\boldsymbol{F}_{ad} = \frac{1}{2}\rho_a U_a^2 d_t C_d(Re_a) \qquad (6) \qquad\qquad \text{where} \qquad Re \equiv \frac{\rho U d_t}{\mu} \qquad (7)$$

The drag forces from the waves are based on the Morison equation [18] given here as Eq. (8), where ρ_w is the density of water, U_w is the velocity of the water, $C_m \equiv 1 + C_a$ is the inertia coefficient, C_a is the added mass coefficient, and A is the acceleration of the fluid in the wave. The wave model is based on linear wave theory or Airy wave theory [19].

$$\boldsymbol{F}_{wd} = \left(\rho_w C_m \frac{\pi}{4} d_m^2 A + \frac{1}{2}\rho_w U_w |U_w| d_m C_d(Re_w) \right) \qquad (8)$$

For both calculations, the coefficient of drag is based on interpolating the experimental results of Roshko [20] with an Akima spline.

The foundation is modelled as a set of linear springs applied to all the nodes within the soil. The equations are based on the model by Arya *et. al.* [21]. Since the Frame3DD structural model cannot model nonlinear forces or springs, this analysis does not have the fidelity required for the nonlinear models recommended by the standards [22], nor the Thieken model [23] that was used to develop the reference design [13] in the scaling tool.

There are some limitations and simplifications in the design analysis. The power spectrum of the waves was not considered in the frequency constraints. Within WISDEM the soil is modelled as linear springs, while the standards recommend nonlinear stiffness models [22]. The depth of the pile could be a design variable that is optimized, but it was set to be equal to the sea depth. The detailed design given by Njomo Wandji [13], the basis of the scaling tool, showed that the monopile diameter design is driven by the fatigue constraint. However, the WISDEM design analysis did not calculate the fatigue damage. Furthermore, the WISDEM analysis did not consider stress concentrations. Another potential manufacturing constraint is the diameter-to-thickness ratio; preliminary analysis showed that this constraint was too restrictive, so it was ignored. Ignoring this constraint could lead to designs that are difficult to manufacture. The maximum thickness constraint was set to 20 *cm* without considering manufacturing limitations. Finally, the transition piece was modelled simply as an added mass between the tower and the monopile. Despite these limitations, WISDEM can still be used to identify important design trends.

3. Site and turbine data

The transition piece height was selected based on a methodology given by Damiani *et. al.* [9], which determines the absolute maximum water surface height during a 1,000-year return period. Based on this analysis and the data on the site [24], the transition piece height was 16.2m for a sea depth of 25 m and 17.1 m for all other sea depths.

The data pertaining to the IEA 10-MW reference wind turbine was obtained from the IEA report [25]. The report provided detailed design data, but did not contain all the information needed for WISDEM. Instead the HAWC2 model and results from the full Design Load Basis (DLB) were used to estimate many of these additional details. For the 15-MW wind turbine

the data within the corresponding report [11] was used, but not all the required data was given here. The missing data for the 15-MW turbine was estimated by scaling the IEA 10-MW data according to the rated power. The frequency limits are based on the range of rotor speeds with a 5% margin. Table 1 summarizes the turbine data used in the WISDEM analysis.

Table 1: Reference wind turbine data

Variable	10-MW Value	15-MW Value
Hub Height m	119	150
Minimum First Frequency Hz	0.1519	0.1323
Maximum First Frequency Hz	0.285	0.2375
RNA Mass kg	$8.64 \cdot 10^5$	$1.017 \cdot 10^6$
RNA Moment of Inertia XX kgm^2	$2.22 \cdot 10^7$	$4.72 \cdot 10^7$
RNA Moment of Inertia YY kgm^2	$1.35 \cdot 10^8$	$2.87 \cdot 10^8$
RNA Moment of Inertia ZZ kgm^2	$1.15 \cdot 10^8$	$2.44 \cdot 10^8$
RNA Product Moment of Inertia XY kgm^2	0.0	0.0
RNA Product Moment of Inertia XZ kgm^2	$7.76 \cdot 10^6$	$1.65 \cdot 10^7$
RNA Product Moment of Inertia YZ kgm^2	0.0	0.0
RNA Center of Gravity m	(-5.986,0.0,3.291)	(-8.057,0.0,4.430)
DLC 1.6 Wind Speed m/s	11.0	10.59
DLC 1.6 Tower Top Force in X kN	$1.91 \cdot 10^3$	$2.86 \cdot 10^3$
DLC 1.6 Tower Top Force in Y kN	$-2.93 \cdot 10^2$	$-4.40 \cdot 10^2$
DLC 1.6 Tower Top Force in Z kN	$-9.12 \cdot 10^3$	$-1.37 \cdot 10^4$
DLC 1.6 Tower Top Moment about X kNm	$1.46 \cdot 10^4$	$2.20 \cdot 10^4$
DLC 1.6 Tower Top Moment about Y kNm	$-6.57 \cdot 10^4$	$-9.85 \cdot 10^4$
DLC 1.6 Tower Top Moment about Z kNm	$-2.42 \cdot 10^4$	$-3.62 \cdot 10^4$
DLC 6.1 Wind Speed m/s	50	50
DLC 6.1 Tower Top Force in X kN	$-1.03 \cdot 10^3$	$-1.54 \cdot 10^3$
DLC 6.1 Tower Top Force in Y kN	$-2.74 \cdot 10^3$	$-4.12 \cdot 10^3$
DLC 6.1 Tower Top Force in Z kN	$-8.79 \cdot 10^3$	$-1.32 \cdot 10^4$
DLC 6.1 Tower Top Moment about X kNm	$1.08 \cdot 10^4$	$1.62 \cdot 10^4$
DLC 6.1 Tower Top Moment about Y kNm	$-7.04 \cdot 10^4$	$-1.06 \cdot 10^5$
DLC 6.1 Tower Top Moment about Z kNm	$4.10 \cdot 10^4$	$6.15 \cdot 10^4$

The site conditions consist of statistics on the wind, wave, water heights and soil properties. The height and the period of the significant wave were taken from the report on the Borssele site [24]. The WISDEM default values were used for the soil properties, and 50 m/s was taken as the 50-year return period. The site properties used in the WISDEM calculation are given in Table 2.

4. Results

4.1. Comparison of the preliminary design methods

The default parameters given in Sec. 3 are used to develop a set of preliminary designs at the water depths of 25 m, 30 m, 35 m and 40 m using both the design tools. The DTU scaling tool does not require the same level of information as the NREL tool (WISDEM). The basis of the DTU scaling tool is in fact a detailed design of a 10-MW reference turbine. The only difference between the original detailed design is that the monopile length is stretched according to the different sea depths.

Fig. 2 shows the diameter variation with height for the 10-MW and 15-MW optimized support structure designs at 40-m water depth. A maximum diameter constraint of 9 m is imposed for

the 10-MW wind turbine, while 10 m is the upper limit for the monopile diameter of the 15-MW turbine. In Sec. 4.3 it is shown that these limits are not far from the results obtained in the unconstrained case for the IEA 10-MW wind turbine. The comparison shows that the DTU scaling tool predicts larger diameters for the 10-MW monopile, while both tools converge to the upper monopile diameter limit for the 15-MW case. Both tools showed little variation in the diameter results across different sea depths, and the essential trends for the 40-m water depth hold.
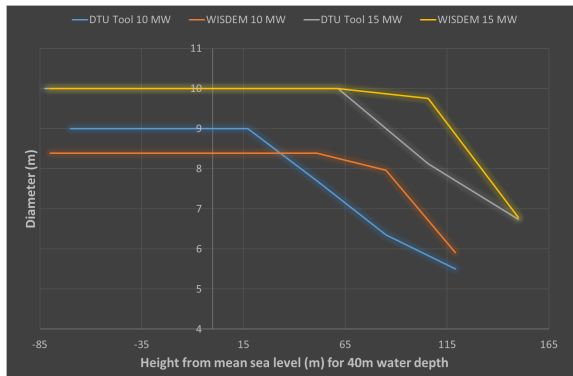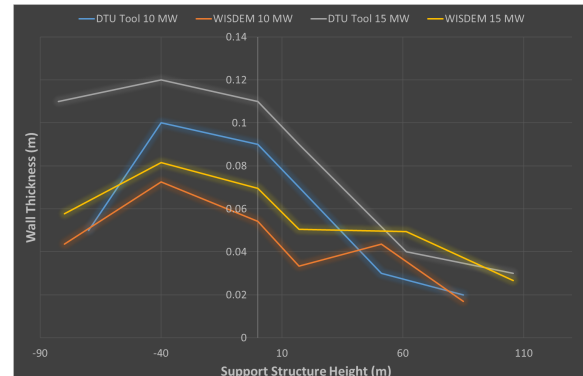

Figure 2: Preliminary diameter comparison

Figure 3: Preliminary thickness comparison

Table 2: Site data used in the WISDEM calculation

Variable	Value
Water Depth m	25,30,35,40
Soil Shear Modulus Pa	$140 \cdot 10^6$
Soil Poisson Ratio	0.4
Steel Youngs Modulus GPa	210
Steel Shear Modulus GPa	80.77
Steel Density kg/m^3	7850
Steel Yield Strength MPa	315
Air Density kg/m^3	1.225
Dynamic Viscosity of Air kg/ms	$1.778 \cdot 10^{-5}$
Water Density kg/m^3	1025
Dynamic Viscosity of Water kg/ms	$1.875 \cdot 10^{-3}$
Significant Wave Height m	6.5
Period of Significant Wave s	12.5
Wind Profile Model	Power-Law
Power Law Shear Exponent	0.14

Fig. 3 shows the thickness of the preliminary designs at 40 m water depth. Similar to the previous results, the DTU scaling tool provides thicker walls for the monopile and thinner walls for the tower compared to the WISDEM results. The maximum thickness is below the soil level, but not at the absolute base of the monopile. The DTU tool does not optimize the wall thickness, but scales it based on the reference 10-MW monopile design. This plot also shows that WISDEM relies heavily on larger wall thicknesses to counteract the increased tower top forces of the 15-MW reference wind turbine. This trend is likely due to the constraint on the maximum diameter, as a larger diameter constraint would have likely lead to smaller wall thickness.

Fig. 4 compares the mass of all the preliminary designs. The results from both optimization tools show very similar mass trends. The DTU scaling tool reference point is based on a high-fidelity detailed design starting point that considered fatigue, stress concentrations and nonlinearities in the soil conditions. The paper by Njomo-Wandj et al. [13] shows that these constraints are driving the design. The WISDEM results may predict lighter designs because important constraints such as fatigue are not included in the optimization. Further investigation is needed in order to determine the role that the optimization and analysis fidelity play in driving the design.
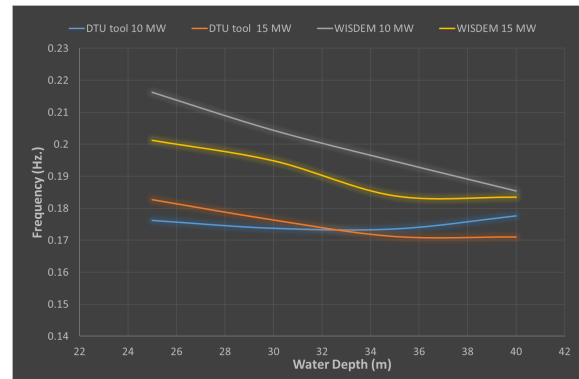
Figure 4: Preliminary mass comparison

Figure 5: Preliminary frequency comparison

Fig. 5 shows the predicted frequencies of the different designs according to the corresponding tool. In both cases, the tools provide designs that have predicted frequencies between the 1P and 3P frequency constraints of the respective turbines.

One advantage of WISDEM is that a physics-based optimization tool provides a lot more information on the constraints. The optimization results highlight the fact that only the global and shell buckling constraints in DLC 6.1 are driving the design optimization. These constraint values are plotted in Fig. 6. The results also show that the shell buckling constraints are no longer active for the 15-MW reference turbine.
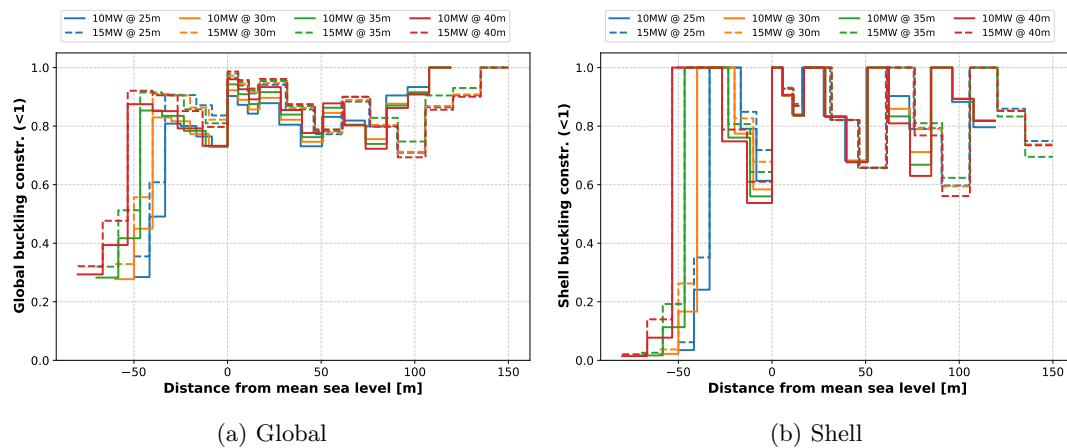

(a) Global

(b) Shell

Figure 6: Comparison of preliminary global and shell buckling estimates with WISDEM

The ease of use within a design process is another important point of comparison between the two tools. The scaling tool only requires a small amount of site and turbine data. Thus it provides results very quickly. The physics-based design optimization tool requires a comparatively large amount of information and more effort for the set up. However, this extra effort leads to a much richer level of information on the performance of the preliminary design and allows for much more design freedom. Furthermore, a lot of the information needed in the optimization would still be required in the detailed design phase. Hence, depending on the application, this extra effort may not be an added cost in the overall design process. A more robust design approach would rely on both approaches, where both the optimization results and

scaling results are compared to ensure that a strong preliminary design candidate is selected for the subsequent detailed design phase. Further development is needed in both approaches though. The scaling tool only depends on the rated power, while the optimization results show that the water depth can drive material thickness in the physics-based design tool. Further development is needed in WISDEM due to the fact that fatigue, stress concentrations and nonlinear soil characteristics are not considered yet.

4.2. The impact of site uncertainty on the design

This parameter uncertainty study looks at parameters that describe the environment. The five parameters that are chosen are the forces applied to the top of the tower, the significant wave height and period, the soil shear stiffness, and the pile depth. The pile depth parameter in principle could be treated as a design variable. However, it was included in the parametric study since it was not explicitly considered as an optimization variable in this work. It is assumed that the parameters can vary between $\pm 20\%$ of their nominal value with a uniform probability. To determine the influence of these parameters on the final design, an uncertainty quantification study is conducted for the following optimized parameters: structural mass, tower and monopile diameter and thickness. The uncertainty quantification is carried out with the Dakota software package [26], using polynomial chaos expansion (PCE) with a sparse grid level of 3 and variance-based decomposition to acquire the Sobol indices. It is important to note that the optimization is nested within the uncertainty quantification analysis. Thus, this study does not assess how a fixed design reacts to uncertainty but rather how the final design reacts to the uncertainty in the input parameters.

Table 3 shows the average and standard deviation normalized by the mean of the different optimization outputs for the various sea depths. Overall, the mass increases from 1.48 to 1.92 $10^6 \ kg$ moving from 25 m to 40 m and has a standard deviation of $\pm 7\%$. The diameter is driven by the maximum diameter constraint for most of the monopile and tower designs, so there is little variance associated to this design parameter. Instead, the optimization uses the thickness to minimize weight and meet the constraints, leading to a larger variance across all thickness design variables. Near the top of the tower, the optimization is varying both the diameter and the thickness. It is also in this region where the greatest variation in the design seems to occur.

Table 3: Optimization output statistics

| Output	Depth 25 m		Depth 30 m		Depth 35 m		Depth 40 m	
	Avg	Std Dev	Avg	Std Dev	Avg	Std Dev	Avg	Std Dev
Structural Mass $10^6 kg$	1.48	7.02%	1.62	7.18%	1.76	7.39%	1.92	7.66%
Monopile Diameter 1 m	7.98	0.74%	7.94	1.67%	7.96	1.06%	7.95	1.16%
Monopile Diameter 2 m	7.98	0.74%	7.94	1.66%	7.96	1.06%	7.95	1.16%
Monopile Diameter 3 m	7.98	0.74%	7.94	1.64%	7.96	1.06%	7.95	1.15%
Monopile Diameter 4 m	7.98	0.74%	7.94	1.64%	7.96	1.06%	7.95	1.15%
Tower Diameter 1 m	7.98	0.72%	7.94	1.64%	7.96	1.06%	7.95	1.15%
Tower Diameter 2 m	7.50	9.13%	7.55	11.89%	7.19	13.99%	7.78	12.08%
Tower Diameter 3 m	5.48	12.22%	5.65	2.93%	5.75	2.65%	5.96	2.36%
Monopile Thickness 1 cm	5.25	7.34%	5.43	7.04%	5.57	7.56%	5.69	8.18%
Monopile Thickness 2 cm	5.81	5.98%	6.02	5.40%	6.20	5.33%	6.37	5.20%
Monopile Thickness 3 cm	4.59	8.20%	4.61	7.61%	4.65	8.38%	4.74	8.33%
Tower Thickness 1 cm	3.95	7.87%	3.95	7.13%	3.94	7.41%	3.95	7.84%
Tower Thickness 2 cm	3.09	16.46%	3.09	6.66%	3.11	6.04%	3.06	6.31%
Tower Thickness 3 cm	2.43	18.71%	2.40	12.18%	2.49	0.03%	2.34	9.66%
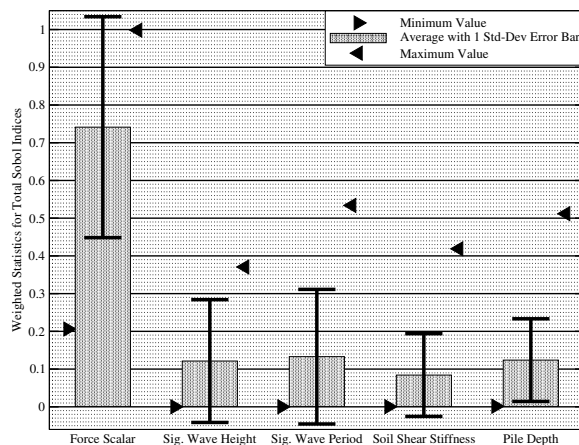
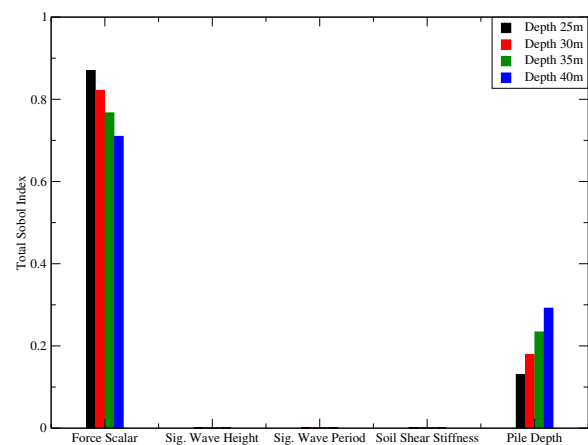Figure 7: Total Sobol index statistics

Figure 8: Total Sobol index for structural mass

To determine the influence of uncertain parameters on the variance, a variance-based decomposition is used to calculate the Sobol indices. The Sobol indices quantify the proportion of the variance of a given output that can be attributed to the variance of a given input. The total indices include the main effects along with all the interaction effects. A large number of Sobol indices are given for each input because there is an index for each output (*i.e.*, the structural mass, diameters and thicknesses). To get an overall sensitivity, the average and standard deviation of the Sobol indices over all outputs are calculated. The Sobol index statistics are weighted according to the variance in Table 3. These results are shown in Fig. 7. The analysis shows that the tower top forces are dominating the design. It should be noted that the assumed uncertainty of the input parameters was arbitrarily set to ±20% and may not reflect the true uncertainty in the field. Regardless, the analysis shows that for very large turbines, the forces generated are so large that they become the most important factor in the design.

Since the mass is an important output for the overall cost, Fig. 8 shows the total Sobol indices associated with this output. It confirms that the variance in the tower top forces is the biggest driver in the mass variance. Since the length of the overall structure contributes to the mass, there is also a secondary sensitivity to the pile depth. It appears that the overall mass is less sensitive to the other environmental conditions.

All the parameters considered in the study affect the forces applied on the structure. The parametric study also shows that the tower top forces govern the optimization-based design, compared to the effect of the other parameters. The forces generated by the turbine grow faster than the other forces acting on the support structure ($\propto R^2$ vs. $\propto R$). Thus, for 10-MW and larger turbines, it appears that the tower top forces have a major influence on the final design. An implication of this is that the other environmental conditions start to have less impact on the design of large turbines and they may require a less detailed evaluation. If the turbine itself has the greatest impact on the support structure design, then large improvements could be achieved if the turbine and support structure are designed together, while there may be diminished benefits for site-specific designs of the support structure.

4.3. Trade-off between mass and maximum diameter

This section is devoted to understanding the trade-off between the mass and the diameter. The former represents a material cost while the later can represent additional costs due to manufacturing, transportation and construction logistics of large scale structures.

4.3.1. Extremes in diameter for the optimal design   The results obtained for the optimization problem of Eq. (5) reveal that the maximum diameter varies with respect to water depth, as shown in Fig. 9. While the results from the two tools are overall in good agreement, the DTU scaling tool shows that for both turbines larger water depths require larger base diameters. The physics-based NREL tool shows the opposite behavior for the 10-MW case. To investigate this further, the basic optimization problem given in Eq. (5) is modified to solve the minimum feasible diameter, as shown in Eq. (9). This study is a precursor to a multi-objective study on the trade-off between structural mass and maximum diameter. The minimum feasible diameter is one extreme of this trade-off. The other extreme is based on solving a problem similar to Eq. (5), except without the maximum diameter constraint. This optimization problem is given in Eq. (10). Both of these optimization problems were solved to determine the extremes of the Pareto front. The resulting Pareto front is further explored in Sec. 4.3.2.

$$
\begin{aligned}
\underset{d_{max}, \boldsymbol{d}_t, \boldsymbol{t}_t, \boldsymbol{d}_m, \boldsymbol{t}_m}{\text{minimize}} \quad & d_{max} \\
\text{s.t.} \quad & 3.87\,m < d < d_{max} \\
& 0.004\,m < t < 0.2\,m \\
& \sigma < \sigma_y \\
& f_{1p} + \delta f < f_{1,2} < f_{3p} - \delta f \\
& n_{s,g} < 1.0
\end{aligned}
\tag{9}
$$

$$
\begin{aligned}
\underset{\boldsymbol{d}_t, \boldsymbol{t}_t, \boldsymbol{d}_m, \boldsymbol{t}_m}{\text{minimize}} \quad & m \\
\text{s.t.} \quad & 0.004\,m < t < 0.2\,m \\
& d > 3.87\,m \\
& \sigma < \sigma_y \\
& f_{1p} + \delta f < f_{1,2} < f_{3p} - \delta f \\
& n_{s,g} < 1.0
\end{aligned}
\tag{10}
$$

4.3.2. WISDEM mass-diameter Pareto front   The Pareto front describes how the mass and maximum diameter vary in an optimal way. It provides a set of optimization solutions where the only way to improve one objective is to worsen the other objective. Herein, the Pareto front is defined by solving problem (5) multiple times while varying the maximum diameter limit between the extremes found in Sec. 4.3.1. The results in Fig. 10 shows that the Pareto front becomes very flat as it approaches the minimum mass solution. As a maximum diameter constraint is introduced and then tightened, additional constraints become active and start to drive the structural mass up faster. This study shows that this effect is gradual enough that the maximum diameter could be reduced by approximately 25% from the optimum value, without having a strong impact on the overall mass.
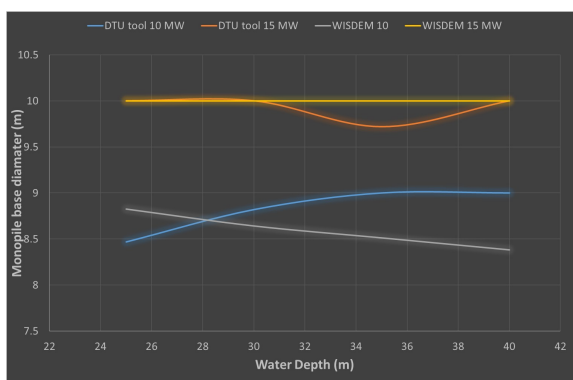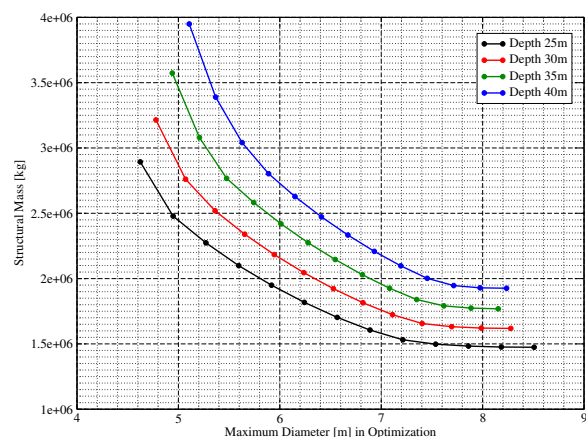

Figure 9: Maximum base diameters

Figure 10: Mass and diameter Pareto front

5. Conclusions

In this work, two different preliminary design methodologies for monopile support structure design are compared, for a range of sea depths and two different turbines (*i.e.*, 10-MW, 15-MW) at the Borssele site III and IV. The optimization results using both WISDEM and the DTU scaling tool are in good agreement, producing lighter support structures satisfying all of the constraints. The scaling tool is based on a detailed reference design that included fatigue and stress concentrations that are not included in the physics-based optimization approach. It is of course an open question to the extent these additional considerations affect the scaled designs.

The results show that monopile diameters up to 9 m are sufficient for the 10-MW wind turbine, whereas the 15-MW turbine requires monopile diameters of at least 10 m. A sensitivity study performed with the optimization-based design approach revealed that the final design is strongly affected by the tower top mass and loads, in comparison to other uncertain site characteristics. This shows that the turbine characteristics are the most important design factors in the range 10–15 MW. Finally, the trade-off between mass and maximum diameter was analyzed. The analysis showed that the maximum diameter can be reduced by approximately 25% from the minimum mass solution without having a strong impact on the overall mass. Thus, there is room for further optimization considering also additional manufacturing and logistic costs for the design of monopile support structures.

6. Future Work

We identified certain areas that could benefit from further development and research. First, the analysis within WISDEM can still be improved in regards to soil modelling and fatigue analysis. Even though the DTU scaling tool is based on a detailed design that included both types of analysis, the optimization results were directly comparable to the WISDEM results. Further investigation is needed to determine the extent to which the different levels of analysis fidelity are affecting the design. Further investigation is also needed to understand why the maximum diameter decreases with water depth in the case of pure mass minimization with WISDEM for the 10-MW turbine case. Since the WISDEM analysis is not based on the same analysis as the scaling tool (*i.e.*, ignores fatigue and a has a simplified soil model), this trend may change once these additional features enter the problem formulation.

There are still a large number of studies that can be conducted in the context of offshore monopile support structure design: A cost model could be used to understand the results from an economic perspective; Fatigue analysis and nonlinear soil models could be incorporated into WISDEM to understand the impact of higher fidelity analysis and additional constraints. Both tools relied on an integrated approach to design simultaneously the tower and monopile. However, a simpler sequential approach could perhaps give similar results between the two approaches (*i.e.*, common tower design for all sea depths), even though some of the results also showed that there is a benefit to designing the turbine and support structure simultaneously in an integrated design process. Additionally, other design processes within the literature should also be compared (*e.g.* [7]). In addition, a soft-soft design could lead to significantly lighter structures. However, this would require detailed analysis to ensure dynamic stability of the final design.

The agreement between the results of the DTU scaling tool and WISDEM shows promise for using either of these models in holistic wind farm design, but further validation is still needed. For both tools, comparison with analysis via a higher fidelity model would help establish their validity. This would then lay the foundation for their use in preliminary monopile design as well as use in broader wind farm layout optimization that seeks to trade-off between energy production, support structure costs and other system costs - to ensure the lowest possible cost of energy for the overall system.

References

[1] Perez-Moreno S S, Dykes K, Merz K O and Zaaijer M B 2018 *Journal of Physics: Conference Series* **1037** 042004

[2] Kallehave D, Byrne B, Thilsted C and Mikkelsen K 2015 *Philosophical transactions. Series A, Mathematical, physical, and engineering sciences* **373**

[3] Muskulus M and Schafhirt S 2014 *Journal of Ocean and Wind Energy* **1** 12–22

[4] Morató A, Sriramula S, Krishnan N and Nichols J 2017 *Renewable Energy* **101** 126–143 ISSN 0960-1481 URL https://www.sciencedirect.com/science/article/pii/S0960148116307662

[5] Velarde J and Bachynski E E 2017 *Energy Procedia* **137** 3–13 ISSN 1876-6102 14th Deep Sea Offshore Wind R&D Conference, EERA DeepWind'2017 URL https://www.sciencedirect.com/science/article/pii/S1876610217352906

[6] Chew K H, Tai K, Ng E and Muskulus M 2016 *Marine Structures* **47** 23–41 ISSN 0951-8339 URL https://www.sciencedirect.com/science/article/pii/S095183391630017X

[7] Arany L, Bhattacharya S, Macdonald J and Hogan S 2017 *Soil Dynamics and Earthquake Engineering* **92** 126 – 152

[8] Dykes K, Graf P, Scott G, Ning A, King R, Guo Y, Parsons T, Damiani R, Felker F and Veers P 2015 *Third Wind Energy Systems Engineering Workshop, Boulder Colorado*

[9] Damiani R, Dykes K and Scott G 2016 *Journal of Physics: Conference Series* **753** 092003

[10] Bortolotti P, Tarres H C, Dykes K, Merz K, Sethuraman L, Verelst D and Zahle F 2019 IEA Wind TCP Task 37: Systems engineering in wind energy - WP2.1 reference wind turbines Tech. Rep. NREL/TP-5000-73492 National Renewable Energy Laboratory

[11] Gaertner E, Rinker J, Sethuraman L, Zahle F, Anderson B, Barter G, Abbas N, Meng F, Bortolotti P, Skrzypinski W, Scott G, Feil R, Bredmose H, Dykes K, Shields M, Allen C and Viselli A 2020 IEA Wind TCP Task 37 - Definition of the IEA wind 15-Megawatt offshore reference wind turbine Tech. rep. National Renewable Energy Laboratory

[12] Allen C, Viselli A, Dagher H, Goupee A, Gaertner E, Abbas N, Hall M and Barter G 2020 IEA Wind TCP Task 37 - Definition of the UMaine VolturnUS-S reference platform developed for the IEA wind 15-Megawatt offshore reference wind turbine Tech. rep. National Renewable Energy Laboratory

[13] Njomo-Wandji W, Natarajan A and Dimitrov N 2019 *Wind Energy* **22** 794–812

[14] Njomo-Wandji W, Natarajan A and Dimitrov N 2018 *Ocean Engineering* **158** 232–252

[15] Gavin H P and Pye J Frame3DD. Static and dynamic structural analysis of 2D and 3D frames http://frame3dd.sourceforge.net/ accessed: 2020-10-20

[16] EN 1993-1-6 1993 Eurocode 3: Design of steel structures—part 1-6: general rules—supplementary rules for the shell structures Tech. rep. European Committee for Standardisation

[17] Germanischer Lloyd 2005 Guideline for the certification of offshore wind turbines. Technical Report IV – Part 2, Chapter 6 Tech. rep. Germanischer Lloyd

[18] Morison J R, Johnson J W and Schaaf S A 1950 *Journal of Petroleum Technology* **2** 149–154

[19] Airy G B 1845 *Tides and Waves* (J.J. Griffin)

[20] Roshko A 1961 *Journal of Fluid Mechanics* **10** 345–356

[21] Arya S C, O'Neill M W and Pincus G 1979 *Design of Structures and Foundations for Vibrating Machines* (Gulf Publishing Company)

[22] Det Norske Veritas 2007 Offshore Standards DNV-OS-J101 – Design of offshore wind turbine structures Tech. rep. Det Norske Veritas

[23] Thieken K, Achmus M and Lemke K 2015 *geotechnik* **38** 267–288

[24] 2019 Borssele wind farm zone wind farm sites III & IV project and site description Tech. rep. Netherlands Enterprise Agency

[25] Bortolotti P, Tarres H C, Dykes K, Merz K, Sethuraman L, Verelst D and Zahle F 2019 IEA Wind TCP Task 37 - Systems engineering in wind energy - WP2.1 reference wind turbines Tech. rep. National Renewable Energy Laboratory

[26] Adams B M, Bohnhoff W J, Dalbey K R, Ebeida M S, Eddy J P, Eldred M S, Hooper R W, Hough P D, Hu K T, Jakeman J D, Khalil M, Maupin K A, Monschke J A, Ridgway E M, Rushdi A A, Seidl D T, Stephens J A, Swiler L P and Winokur J G 2020 Dakota, A multilevel parallel object-oriented framework for design optimization, parameter estimation, uncertainty quantification, and sensitivity analysis: Version 6.12 user's manual Tech. Rep. Sandia Technical Report SAND2020-5001 Sandia National Laboratories